

## Acoustic anomalous reflectors based on diffraction grating engineering

Daniel Torrent\*

*GROC, UJI, Institut de Noves Tecnologies de la Imatge (INIT), Universitat Jaume I, 12071 Castelló, Spain*


(Received 23 April 2018; published 6 August 2018)

We present an efficient method for the design of anomalous reflectors for acoustic waves. The approach is based on the fact that the anomalous reflector is actually a diffraction grating in which the amplitude of all the modes is negligible except for the one traveling towards the desired direction. A supercell of drilled cavities in an acoustically rigid surface is proposed as the basic unit cell, and analytical expressions for an inverse diffraction problem are derived. It is found that the number of cavities required for the realization of an anomalous reflector is equal to the number of diffracted modes to cancel, and this number depends on the relationship between the incident and reflected angles. Then, the “retroreflection” effect is obtained by just one cavity per unit cell; also, with only two cavities it is possible to change the reflection angle of a normally incident wave, and five cavities are enough to design a general retroreflector changing the incident and reflected angles at oblique incidence. Finally, the concept of Snell’s law violation is extended not only to the incident and reflected angles, but also to the plane in which it happens, and a device based on a single cavity in a square lattice is designed in such a way that the reflection plane is rotated  $\pi/4$  with respect to the plane of incidence. Numerical simulations are performed to support the predictions of the analytical expressions, and an excellent agreement is found.

 DOI: [10.1103/PhysRevB.98.060101](https://doi.org/10.1103/PhysRevB.98.060101)

Anomalous reflectors and refractors can be defined as structured flat surfaces in which the relationship between the angles of the incident, reflected, and refracted waves does not satisfy Snell’s law [1]. These devices, designed mainly in the framework of the so-called generalized laws of refraction and reflection [2], have received increasing interest within the last years [3–11], and a wide variety of applications and effects have been envisioned for the control of acoustic waves, such as carpet cloaks [12], acoustic diodes [13], or helical wave-front generators [14].

Also named “gradient metasurfaces,” these devices require a continuous variation of the phase of the fields [2], which in the case of acoustics can be implemented by means of space-coiled scatterers [4] or membranes [12]. Their efficient design requires additionally a specific variation of the impedance of the unit cell [15,16], after a numerical optimization process, since nonlocal effects have to be taken into account. The overall result is that efficient gradient metasurfaces require a complicated design process including a large number of elements per unit cell, which has an obvious practical limitation.

Recently, it has been shown that some functionalities of gradient metasurfaces for electromagnetic or acoustic waves can be achieved by means of properly designed diffraction gratings based on bianisotropic [17–19] or bipartite particles [20,21]. From this perspective, the anomalous reflection or refraction effect consists essentially in canceling all the diffracted modes except for the one traveling towards the desired “anomalous” direction, and this results in the mirage that the wave has not been “diffracted” but “anomalously refracted.” However, current approaches based on diffraction mode control have been applied only to retroreflectors and anomalous reflectors at normal incidence, which will be shown here to be less demanding

than a general anomalous reflector. Additionally, these works still require complex bianisotropic particles to be effective.

In this Rapid Communication, we present a simplified and more general picture for the design of acoustic anomalous reflectors. The approach is based on the efficient engineering of the different diffracted modes by a periodically structured acoustic surface. The structure consists in a perforated acoustically rigid surface, and it is found that the number of cavities per period can be set equal to the number of diffracted modes to be canceled, with the interesting result that only one or two cavities are required for the most typical applications of anomalous reflectors, while only five are required for one of the most challenging applications. Finally, an off-axis anomalous reflector is designed, where the planes of incidence and reflection are different.

The proposed unit cell is shown in Fig. 1(a). It consists of an acoustically rigid surface placed in the  $xy$  plane at  $z = 0$  in which a cluster of  $N$  cavities of length  $L_\alpha$  are drilled and located at the positions  $\mathbf{R}_\alpha$ , for  $\alpha = 1, 2, \dots, N$ . The cross section of the cavities can be arbitrary, but it will be assumed that only the fundamental mode of the waveguide they define is excited [22]. The cavities are backed by a rigid wall, so that no energy is transferred to the other side of the surface. We assume time harmonic dependence of the fields of the form  $e^{-i\omega t}$ . If the surface is excited by an incident plane wave of unitary amplitude and propagating along the  $z$  axis with wave number  $\mathbf{k} = \mathbf{K} + q_0\hat{z}$ , a set of diffracted modes with reflection coefficients  $R_G$  will be excited, so that the pressure and normal velocity fields will be given by

$$P = \sum_G (\delta_{G0} e^{iq_G z} + R_G e^{-iq_G z}) e^{i\mathbf{K}_G \cdot \mathbf{r}}, \quad (1)$$

$$v_n = \frac{iq_G}{k_b Z_b} \sum_G (\delta_{G0} e^{iq_G z} - R_G e^{-iq_G z}) e^{i\mathbf{K}_G \cdot \mathbf{r}}, \quad (2)$$

\* dtorrent@uji.es

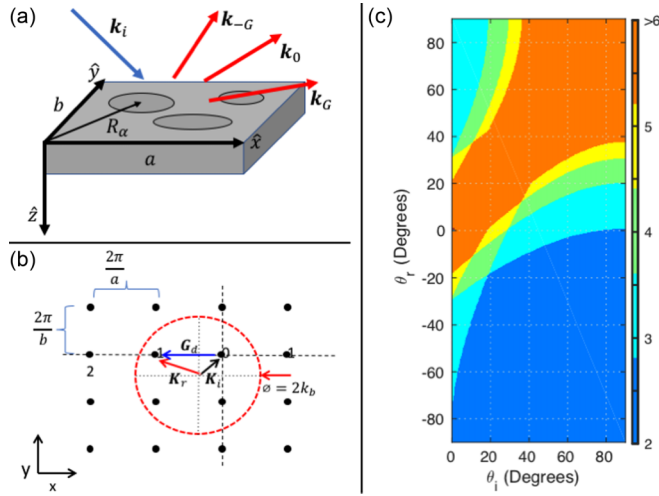


FIG. 1. (a) Schematic representation of the diffraction problem considered in the text. (b) Selection of the grating geometry to generate a desired diffracted mode from a given incident plane wave with in-plane wave vectors  $\mathbf{K}_r$  and  $\mathbf{K}_i$ , respectively. (c) Number of excited diffraction orders for each incident ( $\theta_i$ ) and diffracted ( $\theta_r$ ) angle (defined as the angle of the wave with the  $z$  axis).

where the  $\delta_{0G}$  is the Kronecker delta function and  $|\mathbf{K} + \mathbf{G}|^2 + q_G^2 = \omega^2/c_b^2$ , with  $\mathbf{G}$  being the set of all reciprocal lattice vectors. The reflectance in energy will be always unitary, but we will use the grating to engineer the amount of energy that is transferred to each propagating [ $\text{Im}(q_G) = 0$ ] mode. The fields inside each cavity can be set as [23]

$$P = e^{i\mathbf{K} \cdot \mathbf{R}_\alpha} B_\alpha \frac{\cos k_b(z - L_\alpha)}{\sin k_b L_\alpha}, \quad (3)$$

$$v_n = -\frac{e^{i\mathbf{K} \cdot \mathbf{R}_\alpha}}{Z_b} B_\alpha \frac{\sin k_b(z - L_\alpha)}{\sin k_b L_\alpha}, \quad (4)$$

which ensures the boundary condition  $v_n = 0$  at  $z = L$ .

The mode matching method is applied by projecting the Bloch modes with the  $v_n$  field and the cavity modes for the  $P$  field [23], resulting in the system of equations

$$\sum_{\mathbf{G}} H_{\alpha\mathbf{G}} e^{i\mathbf{G} \cdot \mathbf{R}_\alpha} (\delta_{G0} + R_G) = B_\alpha \cot k_b L_\alpha, \quad (5)$$

$$\delta_{G0} - R_G = -i \frac{k_b}{qG} \sum_{\beta=1}^N f_\beta H_{\beta\mathbf{G}} e^{-i\mathbf{G} \cdot \mathbf{R}_\beta} B_\beta, \quad (6)$$

where the coupling factor is given by  $H_{\alpha\mathbf{G}} = \frac{1}{\Omega_\alpha} \iint_{\Omega_\alpha} e^{i\mathbf{K}\mathbf{G} \cdot (\mathbf{r} - \mathbf{R}_\alpha)} d\Omega$  and the cavity's filling fraction has been defined as  $f_\alpha = \frac{\Omega_\alpha}{\Omega}$ , with  $\Omega$  and  $\Omega_\alpha$  being the areas of the unit cell and the cavity  $\alpha$ , respectively. Solving for  $R_G$  from Eq. (6) and inserting it into (5) leads to a system of equations for the  $B_\alpha$  coefficients,

$$\sum_{\beta=1}^N [\delta_{\alpha\beta} \cot k_b L_\alpha - i \chi_{\alpha\beta}] B_\beta = 2H_{\alpha 0}, \quad (7)$$

where the term  $\chi_{\alpha\beta}$ , which defines the multiple scattering interaction between the cavities in the unit cell, is defined as

$$\chi_{\alpha\beta} = \sum_{\mathbf{G}} \frac{k_b}{qG} H_{\alpha\mathbf{G}} H_{\beta\mathbf{G}} f_\beta e^{-i\mathbf{G} \cdot \mathbf{R}_{\alpha\beta}}. \quad (8)$$

Once the  $B_\alpha$  coefficients are known, the reflection coefficient of each diffracted mode is obtained directly from Eq. (6), solving in this way the full diffraction problem.

However, Eq. (6) can be used to set up an inverse problem as follows: We can impose a set of values for the amplitude of a number  $g$  of diffracted modes  $R_G$ , design a unit cell with  $N = g$  cavities, and solve for the  $B_\alpha$  coefficients from Eq. (6), since it defines a system of  $g$  equations with  $N = g$  unknowns with coefficients  $A_{g\alpha} = f_\beta H_{\beta\mathbf{G}} e^{-i\mathbf{G} \cdot \mathbf{R}_\beta}$ . Once the shapes and positions of the cavities are selected, and solved for the  $B_\alpha$  coefficients, the length of each cavity is directly obtained from Eq. (7) as

$$\cot k_b L_\alpha = \left( 2H_{\alpha 0} + i \sum_{\beta=1}^N \chi_{\alpha\beta} B_\beta \right) B_\alpha^{-1}. \quad (9)$$

Equations (6) and (9) therefore constitute the basis for the inverse design of diffraction gratings, however, it must be pointed out that in order to have a physically acceptable solution, it is required that the right-hand side of the above equation be a real number, since the  $\cot x$  function is real valued for all the physically acceptable  $k_b L_\alpha$  (assuming no loss or gain elements). Therefore, the additional condition

$$\text{Im}(\cot k_b L_\alpha) = 0 \quad (10)$$

has to be satisfied for a physically acceptable solution. In the case of having dissipation in the cavity, the  $\cot x$  function might be inverted in Eq. (9) and impose reality on  $L_\alpha$  instead.

The above procedure considerably simplifies the design of anomalous reflectors, in which it is desired that a wave incident with wave number  $\mathbf{k}_i$  be totally reflected with wave number  $\mathbf{k}_r$ . From a diffraction point of view, this is equivalent to designing a diffraction grating in which the desired reflected wave number corresponds to one of the  $\mathbf{K} + \mathbf{G}$  diffracted modes, and optimizing the grating in such a way that all the other propagating diffracted modes present zero amplitude. The design of the geometry of the lattice is illustrated in Fig. 1(b): We need to impose that the projections of the incident ( $\mathbf{K}_i$ ) and reflected ( $\mathbf{K}_r$ ) wave vectors on the surface satisfy  $|\mathbf{K}_r - \mathbf{K}_i| = \frac{2\pi}{a}$ , to minimize the number of additional diffracted modes (number of points inside the red circle). This condition defines both the lattice orientation and constant  $a$ .

Figure 1(c) shows the number of diffracted modes for all the possible incident and reflection angles with the  $z$  axis,  $\theta_i$  and  $\theta_r$ , respectively. As can be seen, a higher number of diffracted modes is excited for reflection angles similar to the incident angle, while for the ‘‘retroreflection’’ and anomalous reflection effect at normal incidence, only one or two modes are excited and, therefore, they are less demanding devices. This interesting feature of diffraction gratings is that they are responsible for the fact that ‘‘extreme’’ anomalous reflection is easier to implement, although the present approach offers a general method to any configuration.

After selecting the lattice geometry and obtaining the number  $N_d$  of diffracted modes, we set the number of cavities in the unit cell to  $N = N_d - 1$ , since we want to impose  $R_G = 0$  for all the  $N_d$  modes except for  $\mathbf{G} = \frac{2\pi}{a}\hat{x}$ . We will then search for the size and position of the cavities to satisfy condition (10), which will give us the length of the cavities from Eq. (9).

Four examples of the application of the previous approach will be developed. In the first three the anomalous reflection effect will take place in plane, for which a geometry invariant along the  $y$  axis will be selected. In this case, the cavities are grooves in the plate of width  $d_\alpha$ , and we have that  $H_{\alpha G}^{\text{groove}} = \sin(|\mathbf{K} + \mathbf{G}|d_\alpha/2)/(|\mathbf{K} + \mathbf{G}|d_\alpha/2)$ , while for the fourth example a cylindrical cavity of radius  $a_\alpha$  will be employed, and now  $H_{\alpha G}^{\text{cavity}} = 2J_1(|\mathbf{K} + \mathbf{G}|a_\alpha)/(|\mathbf{K} + \mathbf{G}|a_\alpha)$ .

Figure 1(c) shows that the retroreflection effect can be achieved by just two diffracted modes as long as the incident angle  $\theta_i = -\theta_r$  is higher than approximately  $20^\circ$  (dark blue region), therefore we will need only one cavity per unit cell to design such a device. The condition  $R_0 = 0$  in Eq. (6) implies  $B_0 = \frac{iq_0}{f_0 H_0 k_b}$ , and inserting this into Eq. (9) and setting the imaginary part of  $\cot k_b L_0$  equal to zero, we get the condition for energy conservation,

$$\frac{q_{G_d} H_0^2}{q_0 H_{G_d}^2} = 1, \quad (11)$$

which gives us

$$\cot k_b L_0 = \text{Im}(\chi_{00}). \quad (12)$$

Given that in condition (11) the functions  $H_G$  and  $q_G$  are computed at  $\mathbf{K}_i$  ( $\mathbf{G} = 0$ ) and  $\mathbf{K}_r$  ( $\mathbf{G} = -2\pi/a\hat{x}$ ), this condition is trivially satisfied when  $\mathbf{K}_r = -\mathbf{K}_i$ , therefore the design method consists in selecting the width  $d_0$  of the groove and obtaining  $L_0$  from Eq. (12). In our first example we select  $\theta_i = \pi/3$ , so that the retroreflection diffraction condition is satisfied at  $a/\lambda = 2 \sin \theta_i = 1.73$ , and selecting  $d_0 = 0.23a$  defines  $L_0 = 0.23a$ .

Figure 2(a) shows the diffraction energy  $I_G = q_G/q_0 |R_G|^2$  as a function of  $a/\lambda$  for the designed retroreflector. We see how the energy reflected by the fundamental mode (black line) becomes zero and all the energy goes to the first diffraction order (red dashed line) at the desired  $a/\lambda$  point. Figure 2(b) shows the numerical simulations performed with the commercial finite-element software COMSOL MULTIPHYSICS, verifying that the incident (left) and reflected (right) waves have the same propagation direction.

The second example analyzed is the anomalous reflector at normal incidence, in which a wave impinges normally to the surface and it is reflected an angle  $\theta_r$ . In this case, for desired reflection angles higher than  $\pi/6$  we have only three diffracted modes, the fundamental one and the lateral ones at  $\pm\theta_r$ , and the objective is to cancel the fundamental and one of the diffracted orders, so that we need only two grooves per unit cell. We will propose a unit cell in which the two grooves, labeled  $\alpha$  and  $\beta$ , are identical and symmetrically placed in the unit cell,  $x_\beta = -x_\alpha$ , and we will set up this distance by imposing that Eq. (10) be satisfied. The condition  $R_0 = R_G = 0$  now gives  $B_\alpha = \frac{iq_0}{k_b f_0 H_0} \frac{1}{1 - e^{iG x_{\alpha\beta}}}$ , where  $x_{\alpha\beta} = x_\beta - x_\alpha = -2x_\alpha$ .

Figure 3(a) shows the diffracted energy  $I_G$  in this example, where we have selected  $\theta_r = \pi/4$ , which sets  $\lambda/a = 0.7071$ .

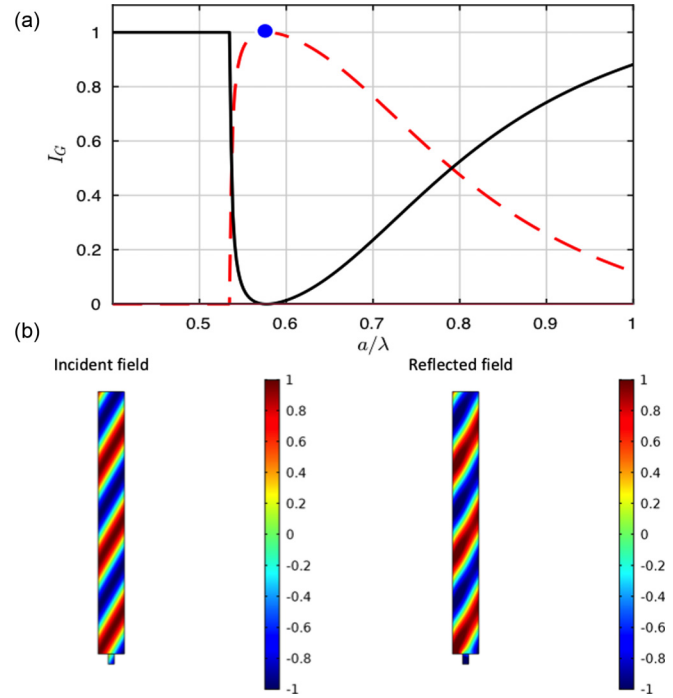


FIG. 2. (a) Diffracted energy as a function of  $a/\lambda$  for the fundamental (black line) and diffracted (red dashed line) modes for a single-groove “retroreflector.” (b) Numerical simulation of the incident (left) and reflected (right) fields, showing the perfect retroreflection effect.

It is clear how the energy of the fundamental (red line) and one diffracted (green dotted-dashed line) modes cancel at the desired wavelength. The width of the grooves is set as

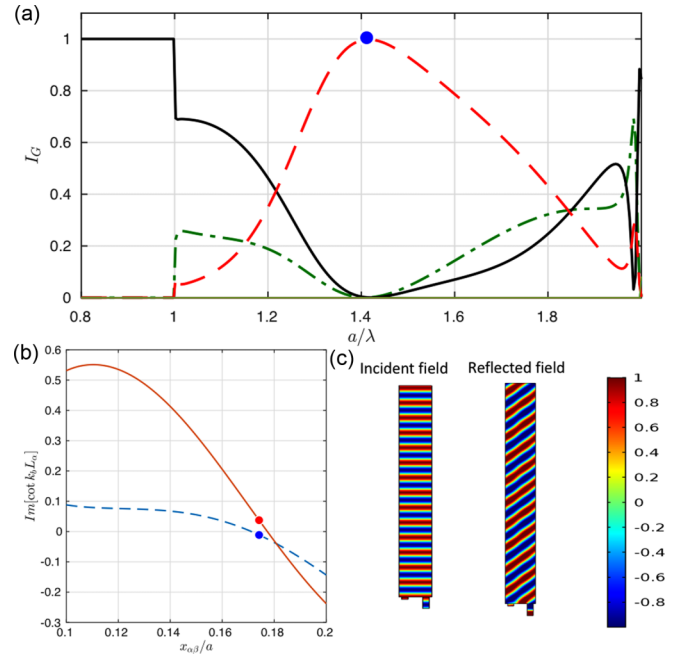


FIG. 3. (a) Diffracted energy as a function of  $a/\lambda$  for each propagating mode for a two-groove anomalous reflector at normal incidence. (b) Plot of  $\text{Im}(\cot k_b L_\alpha)$  as a function of the groove’s semidistance  $x_{\alpha\beta}/a$ , showing the points that satisfy the energy balance condition at  $x_{\alpha\beta} = 0.32a$ . (c) Numerical simulation of the incident (left) and reflected (right) fields.

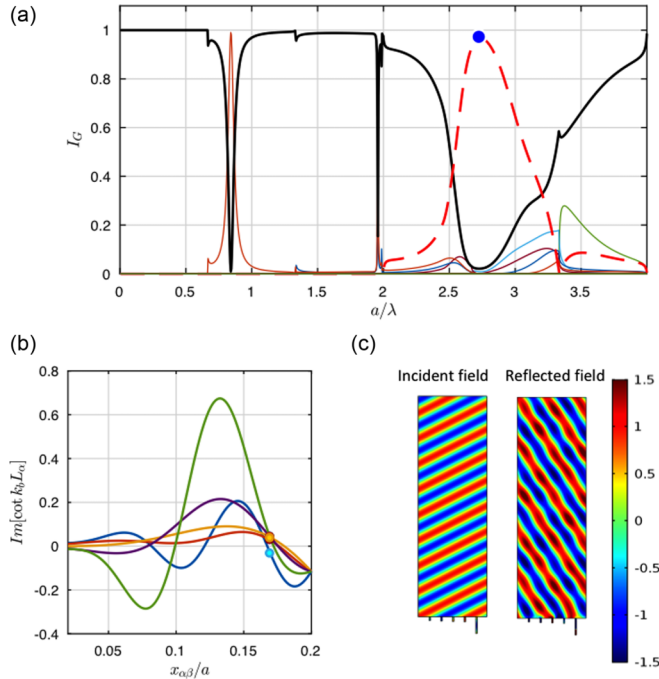


FIG. 4. (a) Diffracted energy as a function of  $a/\lambda$  for each propagating mode for a five-groove anomalous reflector. (b) Plot of  $\text{Im}(\cot k_b L_\alpha)$  as a function of the groove's semidistance  $x_{\alpha\beta}/a$ , showing the points that satisfy the energy balance condition at  $x_{\alpha\beta} = 0.17a$ . (c) Numerical simulation of the incident (left) and reflected (right) fields.

$d_0 = 0.2a$ , and the distance between them is obtained from condition (10), which is plotted in Fig. 3(b) as a function of  $x_{\alpha\beta}/a$ . Finally, the incident and reflected fields computed with COMSOL are depicted in Fig. 3(c).

Next, we show an example of an anomalous reflector, in which the reflection angle of the wave is changed but keeps the same sign. We select  $\theta_i = \pi/3$  and  $\theta_r = \pi/6$ , which correspond to  $N_d = 6$  in Fig. 1(c), therefore this interesting effect can be obtained with only  $N = 5$  grooves. We set the size of the cavity as  $d_0 = 0.02a$  and the  $B_\alpha$  coefficients are directly obtained from the solution of the system of equations defined by Eq. (6). The result of the design can be found in the plot of the diffracted energy in Fig. 4(a), where the distance between grooves  $x_{\alpha\beta} = 0.17a$  that minimizes the imaginary part of  $\cot k_b L_\alpha$  has been obtained from the plot of Fig. 4(b) as in the previous example, and the required lengths of the grooves are  $L_\alpha = 0.0613a, 0.0715a, 0.0776a, 0.0835a,$  and  $0.2775a$ . Figure 4(c) shows the incident  $P_0$  and reflected  $P_S$  waves as simulated with COMSOL, illustrating the nearly perfect performance of the device. It has to be pointed out that the optimal distance between grooves is not  $x_{\alpha\beta} = a/N$ , so that actually the cluster of grooves does not form a sublattice of the main lattice, as it happens in devices based on phase gradients. In other words, in this approach there is no continuous variation of the phase of the fields or the impedance of the surface along the unit cell, but rather it is a diffraction grating engineering that does not take care of the near field and focuses on the amplitude of the propagating fields which is truly responsible for the anomalous reflection effect.

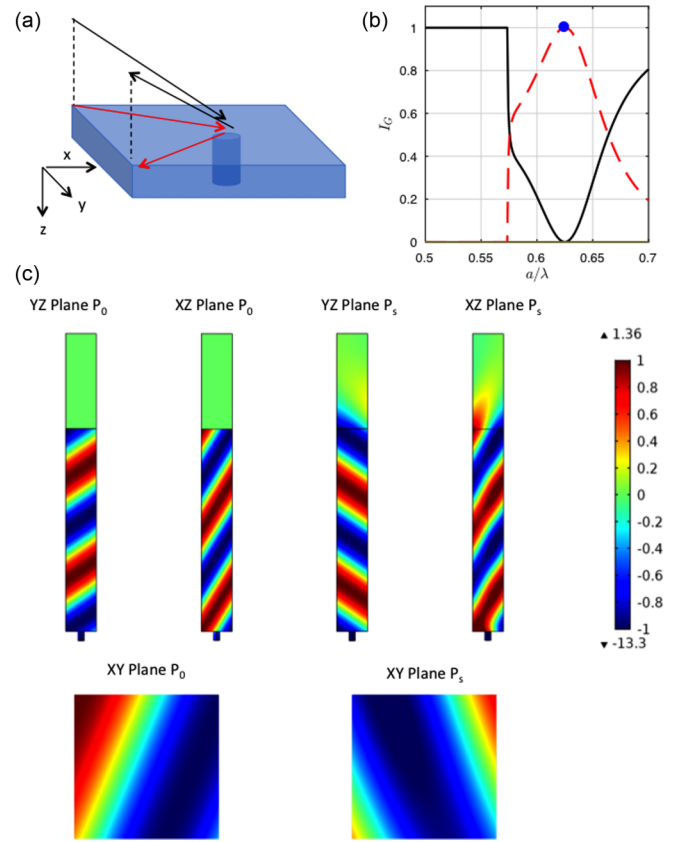


FIG. 5. (a) Geometry of the off-axis reflection problem. (b) Diffracted energy as a function of  $a/\lambda$  for each propagating mode for a reflector made of a single circular cavity in a square unit cell. (c) Projections of the incident and reflected fields at the different planes of the unit cell.

Finally, the presented theory is applied to the design of a four-channel off-axis reflector. This device reflects the incident wave backwards but is rotated a given angle in the  $xy$  plane, as illustrated in Fig. 5(a), therefore the plane of incidence and reflection are different, in contradiction with Snell's law which asserts that these planes have to be the same. We select the incident and reflected angles with the  $z$  axis of  $\theta_i = -\theta_r = \pi/3$  and the rotation angle  $\theta_t = \pi/4$ , where only one cavity per unit cell is required, and selecting circular cavities in a square lattice ensures a four-channel functionality, due to the fourfold symmetry of this lattice. The design method is identical to the retroreflector of Fig. 2, since Eq. (11) is trivially satisfied (the projection of the wave number remains unchanged) and the length of the cylindrical cavity is obtained from Eq. (12). Figure 5(b) shows the diffracted energy and Fig. 5(c) shows the numerical simulations performed with COMSOL of the incident and reflected fields projected at the different sides of the three-dimensional unit cell, showing the retroreflection effect is responsible for the rotation of the reflection plane. The simplicity of this device is remarkable as compared to the equivalent gradient phase metasurface that would be required for this functionality.

In summary, we have shown that anomalous reflection from acoustic surfaces can be properly and efficiently obtained by means of engineered diffraction gratings, in which

subwavelength cavities are drilled in an acoustically rigid surface. The number of cavities required is in general one less than the number of diffracted modes, so that all these modes are canceled except for one, which is the carrier of the wave at the desired reflection angle. It has been shown that unitary efficiency can be achieved for one and two cavities per unit cell, and nearly unitary in the case of five cavities, showing also the great potential that this method has for the design of more efficient anomalous reflectors. This approach presents several advantages in comparison with previous approaches based on gradient index metasurfaces, since no continuous variation of the index or the surface's is required, but just a discrete number of properly selected cavities. The presented

theory therefore opens the door to a different set of devices efficiently designed for the full control of the propagation direction of acoustic waves. Finally, this approach could be applied as well to anomalous refractors and to other domains of physics, such as elasticity or electromagnetism, since the principles on which it is based are general for all type of waves.

Work supported by the LabEx AMADEus (ANR-10-LABX-42) in the framework of IdEx Bordeaux (ANR-10-IDEX-03-02) and by the U.S. Office of Naval Research under Grant No. N00014-17-1-2445. D.T. acknowledges financial support through the “Ramón y Cajal” fellowship.

- 
- [1] M. Born and E. Wolf, *Principles of Optics: Electromagnetic Theory of Propagation, Interference and Diffraction of Light* (Elsevier, Amsterdam, 2013).
- [2] N. Yu, P. Genevet, M. A. Kats, F. Aieta, J.-P. Tetienne, F. Capasso, and Z. Gaburro, *Science* **334**, 333 (2011).
- [3] J. Zhao, B. Li, Z. N. Chen, and C.-W. Qiu, *Appl. Phys. Lett.* **103**, 151604 (2013).
- [4] Y. Li, B. Liang, Z.-m. Gu, X.-y. Zou, and J.-c. Cheng, *Sci. Rep.* **3**, 2546 (2013).
- [5] Y. Li, X. Jiang, R. Q. Li, B. Liang, X. Y. Zou, L. L. Yin, and J. C. Cheng, *Phys. Rev. Appl.* **2**, 064002 (2014).
- [6] G. Ma, M. Yang, S. Xiao, Z. Yang, and P. Sheng, *Nat. Mater.* **13**, 873 (2014).
- [7] Y. Xie, W. Wang, H. Chen, A. Konneker, B.-I. Popa, and S. A. Cummer, *Nat. Commun.* **5**, 5553 (2014).
- [8] K. Tang, C. Qiu, M. Ke, J. Lu, Y. Ye, and Z. Liu, *Sci. Rep.* **4**, 6517 (2014).
- [9] S. Zhai, H. Chen, C. Ding, F. Shen, C. Luo, and X. Zhao, *Appl. Phys. A* **120**, 1283 (2015).
- [10] Y. Li, C. Shen, Y. Xie, J. Li, W. Wang, S. A. Cummer, and Y. Jing, *Phys. Rev. Lett.* **119**, 035501 (2017).
- [11] D.-C. Chen, X.-F. Zhu, Q. Wei, D.-J. Wu, and X.-J. Liu, *J. Appl. Phys.* **123**, 044503 (2018).
- [12] H. Esfahlani, S. Karkar, H. Lissek, and J. R. Mosig, *Phys. Rev. B* **94**, 014302 (2016).
- [13] X.-P. Wang, L.-L. Wan, T.-N. Chen, Q.-X. Liang, and A.-L. Song, *Appl. Phys. Lett.* **109**, 044102 (2016).
- [14] H. Esfahlani, H. Lissek, and J. R. Mosig, *Phys. Rev. B* **95**, 024312 (2017).
- [15] A. Díaz-Rubio and S. A. Tretyakov, *Phys. Rev. B* **96**, 125409 (2017).
- [16] J. Li, C. Shen, A. Díaz-Rubio, S. A. Tretyakov, and S. A. Cummer, *Nat. Commun.* **9**, 1342 (2018).
- [17] Y. Ra'di, D. L. Sounas, and A. Alu, *Phys. Rev. Lett.* **119**, 067404 (2017).
- [18] M. B. Muhlestein, C. F. Sieck, P. S. Wilson, and M. R. Haberman, *Nat. Commun.* **8**, 15625 (2017).
- [19] L. Quan, Y. Ra'di, D. L. Sounas, and A. Alù, *Phys. Rev. Lett.* **120**, 254301 (2018).
- [20] A. M. H. Wong and G. V. Eleftheriades, *Phys. Rev. X* **8**, 011036 (2018).
- [21] D. Sell, J. Yang, E. Wang, T. Phan, S. Doshay, and J. A. Fan, *ACS Photonics* **5**, 2402 (2018).
- [22] J. Christensen, L. Martin-Moreno, and F. J. Garcia-Vidal, *Phys. Rev. Lett.* **101**, 014301 (2008).
- [23] D. Torrent and J. Sánchez-Dehesa, *Phys. Rev. Lett.* **108**, 174301 (2012).